Simple and practical method of characterizing the parametric down-conversion source*

Dong Wang(王东)[1,2,†], Juan Wu(伍娟)[1,2,†], Liang-Yuan Zhao(赵良圆)[1,2], Xue-Bi An(安雪碧)[1,2], Zhen-Qiang Yin(银振强)[1,2,‡], Wei Chen(陈巍)[1,2,‡], Zheng-Fu Han(韩正甫)[1,2,‡], and Qin Wang(王琴)[3,‡]

[1] *Key Laboratory of Quantum Information, University of Science and Technology of China, Hefei* 230026, *China*
[2] *Synergetic Innovation Center of Quantum Information & Quantum Physics, University of Science and Technology of China, Hefei* 230026, *China*
[3] *Institute of Signal Processing and Transmission, Nanjing University of Posts and Telecommunications, Nanjing* 210003, *China*

(Received 20 March 2017; revised manuscript received 23 July 2017; published online 30 September 2017)

Parametric down-conversion (PDC) sources play an important role in quantum information processing, therefore characterizing their properties is necessary. Here we present a statistical model to assess the properties of the PDC source with certain distribution, such as the brightness and photon channel transmissions, we only need to measure the singles and coincidences counts in a few seconds. Furthermore, we validate the model by applying it to a PDC source generating highly non-degenerate photon pairs. The results of the experiment indicate that our method is more simple, efficient, and less time consuming.

Keywords: parametric down-conversion, brightness, photon channel transmission

PACS: 03.67.–a, 42.50.–p, 03.67.Hk, 03.67.Dd **DOI:** 10.1088/1674-1056/26/11/110302

1. Introduction

Single-photon sources (SPS) are the fundamental elements usually used as information carriers in many quantum information processes. To date, many types of alternative single photon sources have been developed, e.g., molecule or atom emission,[1] nitrogen vacancies in diamond,[2] quantum dots,[3] and the parametric down-conversion (PDC) sources.[4] Because of the feasibility and reliability, the PDC sources have been widely adopted in practical implementation of quantum communication, such as long-distance quantum key distribution (QKD),[5–7] quantum repeater,[8] and entanglement swapping.[9]

In the last two decades, PDC sources have been studied extensively, with two typical applications as the heralded single-photon source (HSPS) and the entanglement photon pair source. PDC sources are based on the spontaneous parametric down-conversion (SPDC) process, which possess a probabilistic nature for both the continue-wave (CW) pump[10,11] and pulsed pump[12,13] configurations. As a result, the photons emitted from the PDC sources follow a certain statistical distribution such as Poisson or thermal distribution, which can be achieved by properly adjusting the experimental set-up.[14] Nevertheless, the pulsed pumping regime has more advantages over the CW one, for providing the time information of the emitted photons, which can be very useful in quantum communications.

It is necessary to know the properties of the PDC source in most applications. For instance, when a PDC source is applied to a QKD system, it can generate the decoy-state either actively or passively,[15–18] dramatically increasing the security of realistic QKD. In those protocols, it is important to know the brightness (i.e., the mean photon number per time unit) and the photon channel transmissions to estimate the key generation rate. Unfortunately, the realistic PDC sources suffer from the lossy channels, inefficient single mode fiber coupling, and non photon-number-resolving detectors. All these factors lead to the assessment of the source brightness being a difficult task. Consequently, efforts have been made to characterize the PDC sources.[19,20] The method in Ref. [19] is related to the CW pump regime, while the method in Ref. [20] is related to the pulsed one. Both methods are less practical for their complexity. Hence, a more simple and straightforward method is needed to assess the properties of the PDC sources in practical quantum information processing.

Here we propose a model of the pulsed pump PDC source, and derive the analytic formulas for the single and coincidence counting rates, which are the functions of the bright-

*Project supported by the Strategic Priority Research Program (B) of the Chinese Academy of Sciences (CAS) (Grant Nos. XDB01030100 and XDB01030300), the National Key Research and Development Program of China (Grant No. 2016YFA0302600), and the National Natural Science Foundation of China (Grant Nos. 61475148 and 61575183).

†These authors contributed equally to this work and should be considered co-first authors.
‡Corresponding author. E-mail: yinzheqi@mail.ustc.edu.cn
‡Corresponding author. E-mail: weich@ustc.edu.cn
‡Corresponding author. E-mail: zfhan@ustc.edu.cn
‡Corresponding author. E-mail: qinw@njut.edu.cn

© 2017 Chinese Physical Society and IOP Publishing Ltd

ness and the transmittance. The coincidence counting rates include the total, the real, the accidental, and the side peak ones. Then by substituting the measured values into the statistical model of the single and the coincidences counts, one can simply and quickly calculate all the parameters that are needed, such as the brightness and the total efficiency of each photon channel. Moreover, with the measured single and coincidence counts in a Hanbury–Brown–Twiss (HBT) experiment,[21] one can obtain the second-order autocorrelation function $g^2(0)$. We experimentally verify our model by using a PPLN based non-degenerate PDC source; with the measured single counting rate and coincidence counting rate, we estimate the brightness and the photon channel transmissions; and then, we predict the real and accidental coincidence counting rates. We finally measure the heralded second-order autocorrelation function, which indicates that our source is very close to the single-photon source.

2. Statistical model of the PDC source

According to the probabilistic nature of the PDC source, we develop a statistical model to access the properties of the sources. A simple model of the PDC source is shown in Fig. 1. As shown in Fig. 1, one pump photon is focused on a nonlinear crystal (NC). After the spontaneous parametric down-conversion process, a photon pair which includes a signal photon and an idler photon maybe generated simultaneously. Then the photon pair is separated by a dichroic mirror (DM) in the case of collinear generation with non-degenerate wavelengths, and individually collected into fibers by a coupler. The idler photon is directly detected by the single photon detector D_1. While the signal photon is sent into a 50/50 fiber beam splitter (FBS) and detected by two single photon detectors D_2 and D_3, respectively. It should be noted that the FBS is not necessary in determining the source brightness and photon channel transmission, which is only used to perform the HBT experiment and measure the second-order autocorrelation function $g^2(0)$.

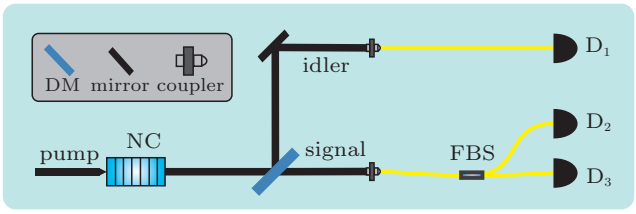


Fig. 1. (color online) The model of SPDC source.

2.1. Single and coincidences counts

Since all the counts are detected within a time window either in a CW or a pulsed laser scheme, in the following for a convenient description, we suppose a pulsed laser scheme with a repetition rate of f. Assume that the mean photon number of photon pairs emitted per pulse from the crystal is μ_0. Denote the dark count rate of each detector as d_i $(i = 1,2,3)$, and the transmission efficiency of each mode as η_i. Here η_i includes all the optical efficiency, the fiber coupling efficiency, and the efficiency of the detectors. According to our statistical model, the singles and any kind of coincidence can be easily deduced as follows.

Single counting rate For an n-photon pair state generated from the PDC source, the yield of the detector D_i for each photon pair state can be written as

$$Y_i = 1 - (1 - d_i)(1 - \eta_i)^n. \tag{1}$$

Then the counting rate of detector D_i can be expressed as

$$R_i = f \sum_{n=0}^{\infty} Y_i P_n(\mu_0), \tag{2}$$

where $P_n(\mu_0)$ is the photon number distribution.

Total coincidence counting rate In our model, one should measure the total coincidence between detectors D_1 and D_j $(j = 2,3)$, which includes the real coincidence and the accidental coincidence. As is known, the coincidence is obtained when the two detectors click simultaneously within the same time window. The yield of the detector for each pulse is already given by Eq. (1), then we can easily obtain the total coincidence counting rate

$$C_{1j}^{\mathrm{t}} = f \sum_{n=0}^{\infty} Y_1 Y_j P_n(\mu_0), \quad (j = 2,3). \tag{3}$$

Real coincidence counting rates The real coincidence comes from the case that the idler and one path of the signal photon from the same n-photon pair are simultaneously detected, its yield is given by

$$Y_{1j}^{\mathrm{rc}} = \sum_{p=1}^{n} \sum_{q=1}^{p} C_n^p \eta_1{}^p (1 - \eta_1)^{n-p} C_p^q \eta_j{}^q (1 - \eta_j)^{p-q}, \tag{4}$$

where "rc" indicates the real coincidence, and "q" shows that the photon pair participates in the coincidence. Furthermore, the counting rate of real coincidence can be obtained in the same way

$$C_{1j}^{\mathrm{r}} = f \sum_{n=1}^{\infty} Y_{1j}^{\mathrm{rc}} P_n(\mu_0), \quad (j = 2,3). \tag{5}$$

Accidental coincidence counting rate As for the accidental coincidence, it can be divided into four classes: (i) the click events of detectors D_1 and D_j are both from the dark counts; (ii) D_1 click is caused by the dark counts, and D_j is caused by the PDC photons; (iii) D_j click is caused by the dark counts, and D_1 is caused by the PDC photons; (iv) the detected photons of D_1 and D_j come from different PDC photon pairs. Therefore, the accidental coincidence can be given as

$$C_{1j}^{\mathrm{a}} = f\{d_1 d_j \sum_{n=0}^{\infty} (1 - \eta_1)^n (1 - \eta_j)^n P_n(\mu_0)$$

$$
\begin{aligned}
&+ d_j \sum_{n=1}^{\infty} \sum_{m=1}^{n} C_n^m \eta_1^m (1-\eta_1)^{n-m} (1-\eta_j)^n P_n(\mu_0) \\
&+ \sum_{n=2}^{\infty} \sum_{p=1}^{n-1} \sum_{q=1}^{p} C_n^m \eta_1^p \\
&\times (1-\eta_1)^{n-p} C_{n-p}^q \eta_j^q (1-\eta_j)^{n-q} P_n(\mu_0) \\
&+ d_1 \sum_{n=1}^{\infty} \sum_{m=1}^{n} C_n^m \eta_j^m (1-\eta_j)^{n-m} \\
&\times (1-\eta_j)^n P_n(\mu_0)\}, \quad (j=2,3). \qquad (6)
\end{aligned}
$$

Side peak coincidence counting rates If the relative delay between two paths is adjusted to around k/f ($k = 1,2,3,\ldots$), the coincidence can still be measured, which is called the side peak coincidence. This coincidence comes from two independent pulses, therefore the corresponding expression is

$$
\begin{aligned}
C_{1j}^{\mathrm{s}} &= f \sum_{m=0}^{\infty} Y_1 P_m(\mu_0) \sum_{n=0}^{\infty} Y_j P_n(\mu_0) \\
&= \frac{R_1 R_j}{f}, \quad (j=2,3). \qquad (7)
\end{aligned}
$$

From the above deduction, we can arrive at three conclusions. First, the singles, the total and side peak coincidence counting rates can be measured directly from an experiment, we can use the measured counting values to assess the brightness and efficiency. Second, it has been proven through Mathematica that the sum of the real and accidental coincidence counting rates is exactly equal to the total coincidence, i.e., $C_{1j}^{\mathrm{r}} + C_{1j}^{\mathrm{a}} = C_{1j}^{\mathrm{t}}$, which in turn validates our model. Third, the accidental and side peak coincidences are not the same thing.

2.2. Brightness and photon channel transmission

Note that our statistical model can apply to any certain photon number distribution of the PDC source. If we have a prior knowledge of the photon number distribution, then we can determine the brightness (μ_0) and photon channel transmission (η_i) by just measuring the single and total coincidence counting rates. Now we take the typical Poisson and thermal distributions for examples.

The Poisson distribution can be expressed as $P_n(\mu_0) = (\mathrm{e}^{-\mu_0}\mu_0^n)/n!$, therefore the expressions (2) and (3) can be further simplified as

$$
\begin{aligned}
R_i &= f[1-(1-d_i)\mathrm{e}^{-\mu_0\eta_i}], \quad (i=1,2,3; j=2,3), \\
C_{1j}^{\mathrm{t}} &= f[1-(1-d_1)\mathrm{e}^{-\mu_0\eta_1} - (1-d_j)\mathrm{e}^{-\mu_0\eta_j} \\
&\quad + (1-d_1)(1-d_j)\mathrm{e}^{-\mu_0(\eta_1+\eta_j-\eta_1\eta_j)}]. \qquad (8)
\end{aligned}
$$

The thermal distribution is $P_n(\mu_0) = \mu_0^n/(1+\mu_0)^{n+1}$, then expressions (2) and (3) can be given by

$$
\begin{aligned}
R_i &= f\left(1 - \frac{1-d_i}{1+\mu_0\eta_i}\right), \quad (i=1,2,3; j=2,3), \\
C_{1j}^{\mathrm{t}} &= f\left[1 - \frac{1-d_1}{1+\mu_0\eta_1} - \frac{1-d_j}{1+\mu_0\eta_j} \right. \\
&\quad \left. + \frac{(1-d_1)(1-d_j)}{1+\mu_0\eta_1+\mu_0\eta_j-\mu_0\eta_1\eta_j}\right]. \qquad (9)
\end{aligned}
$$

Finally, after substituting the measured dark count rate d_i, and with the measured single and total coincidence counting rates, μ_0 and η_i can be numerically solved.

Particularly if the condition $\mu_0\eta_i \ll 1$ is satisfied, and the dark count rate can be neglected, for both distributions we can obtain the further simplified results

$$
\begin{aligned}
R_i &= f\mu_0\eta_i, \quad (i=1,2,3), \\
C_{1j}^{\mathrm{t}} &= f\mu_0\eta_1\eta_j, \quad C_{1j}^{\mathrm{s}} = f\mu_0^2\eta_1\eta_j, \quad (j=2,3). \qquad (10)
\end{aligned}
$$

The μ_0 and η_i can also be simply obtained. Equation (10) indicates that the singles and total coincidence are proportional to μ_0, while the side peak coincidence is in proportion to μ_0^2.

2.3. The second-order autocorrelation function $g^2(0)$

The second-order autocorrelation function can be found via an HBT experiment by measuring the three-path coincidence using three detectors (D_1, D_2, and D_3), as shown in Fig. 1. For any photon number distribution, the second-order autocorrelation function[22] has always been expressed as

$$
g^{(2)}(\tau=0) = \frac{C_{23} f}{R_2 R_3}, \qquad (11)
$$

and the heralded second-order autocorrelation function[23] can be obtained by

$$
g_{\mathrm{H}}^{(2)}(0) = \frac{2C_{123}R_1}{(C_{12}^{\mathrm{t}} + C_{13}^{\mathrm{t}})^2}, \qquad (12)
$$

where C_{23} is the coincidence counting rate of D_2 and D_3, and C_{123} is the coincidence counting rate of D_1, D_2, and D_3. Here, we also take the Poisson and thermal distributions for examples to discuss the distribution of the second-order autocorrelation function.

For the Poisson distribution, when the delay of the two path (τ) is 0, the coincidence between D_2 and D_3 is given by

$$
\begin{aligned}
C_{23} &= f \sum_{n=0}^{\infty} \sum_{m=0}^{n} C_n^m t^m (1-t)^{n-m} [1-(1-d_2)(1-\eta_{20})^m] \\
&\quad \times \left[1-(1-d_3)(1-\eta_{30})^{n-m}\right] \frac{\mu_0^n}{n!} \mathrm{e}^{-\mu_0} \\
&= f[1-(1-d_2)\,\mathrm{e}^{-\mu_0\eta_2}][1-(1-d_3)\,\mathrm{e}^{-\mu_0\eta_3}] \\
&= R_2 R_3 / f, \qquad (13)
\end{aligned}
$$

where t is the transmittance of the FBS, $\eta_2 = t\eta_{20}$, and $\eta_3 = (1-t)\eta_{30}$. Then $g^{(2)}(\tau=0)$ is estimated by

$$
g^{(2)}(\tau=0) = \frac{C_{23} f}{R_2 R_3} = 1. \qquad (14)
$$

This result indicates that $g^{(2)}(0)$ is independent of the brightness.

For the thermal distribution, the coincidence between D_2 and D_3 when $\tau = 0$ can be obtained in a similar way

$$\begin{aligned} C_{23} &= f\sum_{n=0}^{\infty}\sum_{m=0}^{n} C_n^m t^m (1-t)^{n-m}[1-(1-d_2)(1-\eta_{20})^m] \\ &\quad \times [1-(1-d_3)(1-\eta_{30})^{n-m}]\frac{\mu_0^n}{(1+\mu_0)^n} \\ &= f\left(1-\frac{1-d_2}{1+\mu_0\eta_2}\right)\left(1-\frac{1-d_3}{1+\mu_0\eta_3}\right) \\ &\quad + \frac{f(1-d_2)(1-d_3)\mu_0^2\eta_2\eta_3}{(1+\mu_0\eta_2)(1+\mu_0\eta_3)(1+\mu_0\eta_2+\mu_0\eta_3)} \\ &= \frac{R_2R_3}{f} + \frac{(f-R_2)(f-R_3)(R_2-d_2f)(R_3-d_3f)}{f[(1-d_2-d_3)f^2+(d_2R_3+d_3R_2)f-R_2R_3]}. \end{aligned} \tag{15}$$

When neglecting the dark count rate, we can obtain an approximated result

$$C_{23} = \frac{R_2R_3}{f}\left[1+\frac{(f-R_2)(f-R_3)}{f^2-R_2R_3}\right]. \tag{16}$$

Therefore the second-order autocorrelation function for the thermal distribution is

$$\begin{aligned} g^{(2)}(\tau=0) &= \frac{C_{23}f}{R_2R_3} = 1+\frac{(f-R_2)(f-R_3)}{f^2-R_2R_3} \\ &= 1+\frac{1}{1+\mu_0(\eta_2+\eta_3)}. \end{aligned} \tag{17}$$

With $\mu_0, \eta_2, \eta_3 \geqslant 0$, we can obtain the following relationship:

$$1 < g^{(2)}(\tau=0) \leqslant 2. \tag{18}$$

From the above derivation, we can easily see that $g^2(0) = 0$ implies a perfect single photon source. However, due to the disturbance from external experiment conditions, we usually regard it as achieving an HSPS when $g^2(0) < 1$. Alternatively, $g^2(0) \geq 1$ describes a classical source (for Poisson $g^2(0) = 1$ and for thermal $1 < g^2(0) \leq 2$).

3. Experimental results

A schematic of our experimental setup is displayed in Fig. 2. A 76 MHz repetition rate, picosecond, mode-locked Ti:sapphire laser at 898 nm is frequency doubled into 449 nm light through a β-BaB_2O_4 (BBO) crystal. It is then used to pump a periodically poled $LiNbO_3$ (PPLN) crystal, generating nondegenerated parametric down-conversion photon pairs centered at 633 nm and 1545 nm, respectively. The generated photon pairs are separated by a dichroic mirror (DM). Photons at 1545 nm are further split into two paths by a fiber beam splitter (FBS). Then each path is individually coupled into a fiber and filtered by a tunable bandpass filter with full width half maximum of 3 nm. The photons in the two paths are finally sent into home-made super-conducting nanowire single-photon detectors (SNSPD) operating at 2.15 K with a 55% detection efficiency and a dark count rate of 16 Hz. Moreover, two polarization controllers (PC) are placed in front of the SNSPDs to maximize the counting rates. Photons at 633 nm are coupled into a fiber and sent into a silicon avalanche photo diode (SAPD). We use a time-to-digital converter (TDC) to collect the signals from all detectors. The start signal of TDC comes from the clock of the Ti:sapphire laser, which is frequency divided into 380 kHz. The time window is set to 3 ns.

First, we performed the HBT experiment, measuring the single counting rates of D_2 and D_3 and their coincidence counting rate C_{23}. Here, we only discuss the Poisson distribution, $g^{(2)}(0)$ is calculated to be 1.022 ± 0.004 using Eq. (11). This result demonstrates that the photon number distribution follows the Poisson distribution. The single counts and the

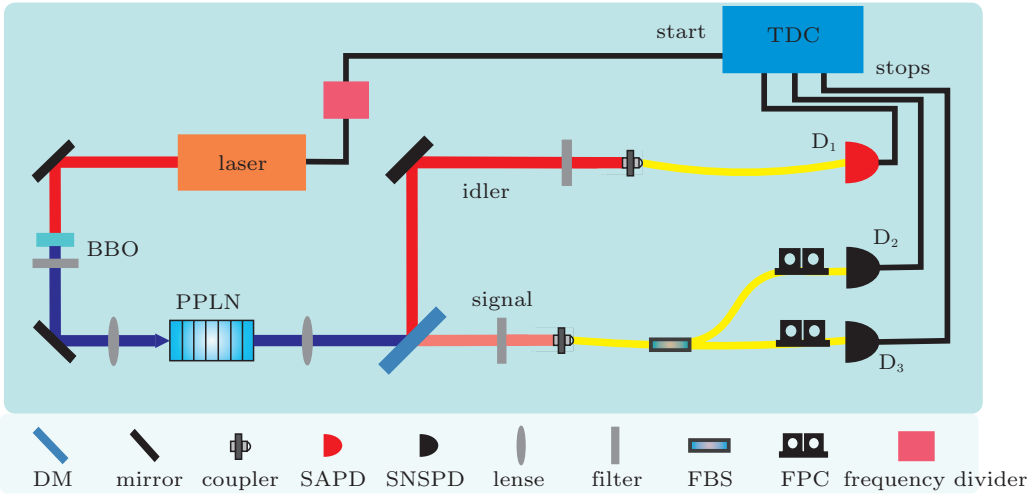


Fig. 2. (color online) The experimental setup of SPDC source.

total coincidences were measured with pump powers set to 100 μW, 200 μW, 300 μW, 400 μW, and 500 μW, respectively. The measured R_1, C^{t}_{12} and C^{t}_{13} are displayed in Fig. 3(a). C^{s}_{12} and C^{s}_{13} are shown in Fig. 3(b). By using our model for the Poisson distribution, we can calculate the mean photon number μ_0 and photon channel transmissions η_i $(i=1,2,3)$, which are demonstrated in Figs. 4(a) and 4(b), respectively.

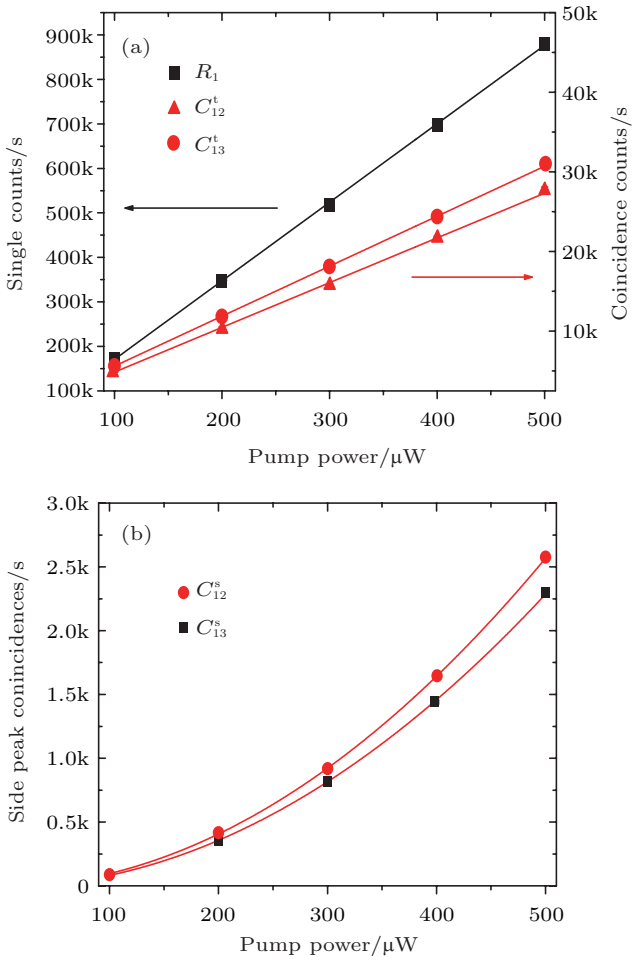


Fig. 3. (a) The measured single count rate of D_1, total coincidences between D_1, D_2 and D_1, D_3 for different pump power. (b) Side peak coincidences between D_1, D_2 and D_1, D_3 for different pump power.

From Fig. 3(a), we can see that the experimental data of R_1, C^{t}_{12}, and C^{t}_{13} can be well linearly fitted, which is in agreement with Eq. (10). Similarly, figure 3(b) shows that the experimental data of C^{s}_{12} and C^{s}_{13} can perfectly match the quadric curve described by Eq. (10). It should be emphasized that all the fittings rely on the condition $\mu_0\eta_i \ll 1$; in our experiment, they are estimated to be $\eta_1 = 11.24\%$, $\eta_2 = 2.87\%$, $\eta_3 = 3.26\%$, together with the value of μ_0, the condition can be surely satisfied.

Figure 4(a) demonstrates a proportionality between the pump power and the generated mean photon number μ_0. We can figure out from Fig. 4(b) that the calculated photon channel transmissions do not change with the pump power, which manifests a reliability of our model.

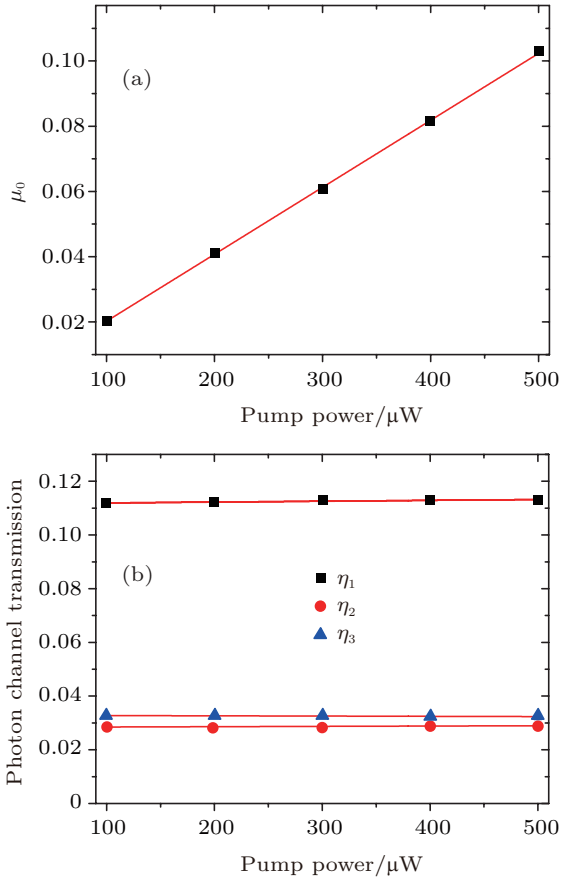


Fig. 4. (color online) (a) The mean photon number per pulse generated by the crystal with increasing pump power. (b) The photon channel transmission with increasing pump power.

With the estimated values of μ_0 and η_i $(i=1,2,3)$, substituting the Poisson distribution into Eqs. (5) and (9), we can predict the real and accidental coincidences. The expressions are

$$\begin{aligned} C^{r}_{1j} &= f(1-e^{-\mu_0\eta_1\eta_j}),(j=2,3),\\ C^{a}_{1j} &= f e^{-\mu_0\eta_1\eta_j}[1-(1-d_1)e^{-\mu_0\eta_1(1-\eta_j)}]\\ &\quad\times[1-(1-d_j)e^{-\mu_0\eta_j(1-\eta_1)}]. \end{aligned} \tag{19}$$

The predicted C^{r}_{1j} and C^{a}_{1j} versus μ_0 according to Eq. (19) are shown in Fig. 5. It is obviously in Fig. 5 that the predicted real and accidental coincidences have the linear and quadratic relationships with the mean photon number, respectively. This is in accord with the approximate results under the condition of $\mu_0\eta_i \ll 1$.

By measuring the single counting rates R_1 and the coincidence counting rates C_{12}, C_{13}, C_{123} together with Eq. (12), we can obtain the heralded second-order autocorrelation function $g^{(2)}_{H}(0)$ at different pump powers. Figure 6 shows $g^{(2)}_{H}(0)$ as a function of the pump power. When the mean photon number is kept less than 0.1 as in our experiment, the probability of single photon is much larger than that of multi-photon. What is more, after being heralded, the vacuum pulse can be largely eliminated, and so the single photon becomes the dominant part in the source. Therefore, the second-order autocorrelation

function measured under the condition that the idler detector clicks can be very close to that of a single-photon source.

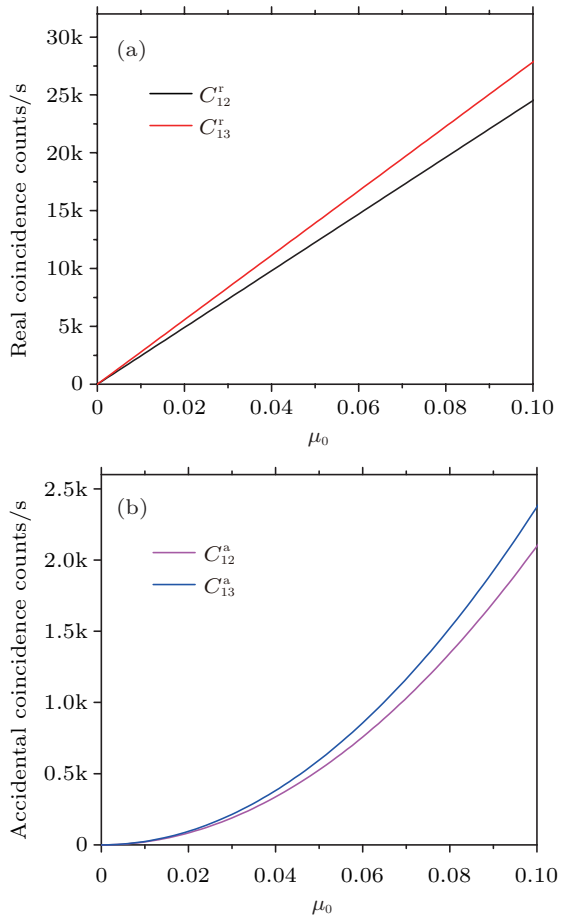


Fig. 5. (color online) (a) The predicted real coincidences between D_1, D_2 and D_1, D_3. (b) The predicted accidental coincidences between D_1, D_2 and D_1, D_3.

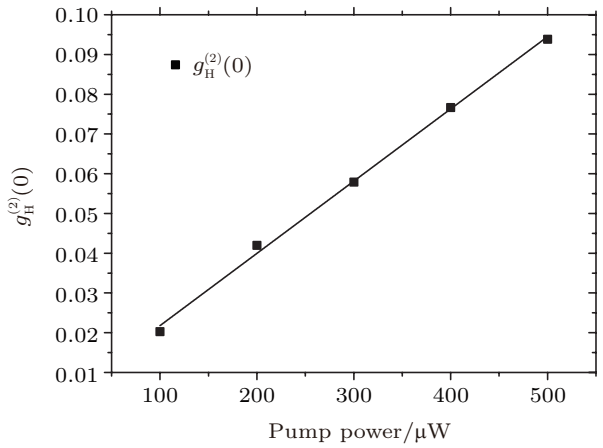


Fig. 6. The heralded second-order autocorrelation function measured at different pump powers.

4. Conclusion

We proposed a simple statistical model to characterize a PDC source, which provides the means to estimate the brightness, photon number transmissions, and the second-order autocorrelation function by measuring the single counts and total coincidence counts. Moreover, with the estimated photon channel transmission and mean photon number per pulse, one can predict the real and accidental coincidence counts. We constructed a PDC source and characterized its properties by using our method, the experimental results confirmed our statistical model. This analysis method is simple and less time consuming in accessing a PDC source, which we believe will have a wide application in the field of quantum communication.

References

[1] Lounis B and Moerner W E 2000 *Nature* **407** 491
[2] Kurtsiefer C, Mayer S, Zarda P and Weinfurter H 2000 *Phys. Rev. Lett.* **85** 290
[3] Pelton M, Santori C, Vuckovic J, Zhang B, Solomon G S, Plant J and Yamamoto Y 2002 *Phys. Rev. Lett.* **89** 233602
[4] Burnham D C and Weinberg D L 1970 *Phys. Rev. Lett.* **25** 84
[5] Bennett C H and Brassard G 1984 *Proceedings of the IEEE International Conference on Computers, Systems, and Signal Processing* pp. 175–179
[6] Ekert A 1991 *Phys. Rev. Lett.* **67** 661
[7] Gisin N, Ribordy G, Tittel W and Zbinden H 2002 *Rev. Mod. Phys.* **74** 145
[8] Briegel H J, Dür W, Cirac J I and Zoller P 1998 *Phys. Rev. Lett.* **81** 5932
[9] Pan J W, Bouwmeester D, Weinfurter H and Zeilinger A 1998 *Phys. Rev. Lett.* **80** 3891
[10] Fasel S, Alibart O, Tanzilli S, Baldi P, Beveratos A, Gisin N and Zbinden H 2004 *New J. Phys.* **6** 163
[11] Alibart O, Ostrowsky D B, Baldi P and Tanzilli S 2005 *Opt. Lett.* **30** 1539
[12] Pittman T B, Jacobs B C and Franson J D 2005 *Opt. Commun.* **246** 545
[13] Castelletto S, Degiovanni I P, Schettini V and Migdall A 2005 *Opt. Express* **13** 6709
[14] Riedmatten H D, Scarani V, Marcikic I, Acín A, Tittel W, Zbinden H and Gisin N 2004 *J. Mod. Opt.* **51** 1637
[15] Adachi Y, Yamamoto T, Koashi M and Imoto N 2007 *Phys. Rev. lett.* **99** 180503
[16] Ma X F and Lo H K 2008 *New J. Phys.* **10** 073018
[17] Hu J Z and Wang X B 2010 arXiv:1004.3730v2
[18] Wang Q, Zhang C H and Wang X B 2016 *Phys. Rev. A* **93** 032312
[19] Tengner M and Ljunggren D 2007 arXiv:0706.2985v1[quant-ph]
[20] Bussieres F, Slater J A, Godbout N and Tittel W 2008 *Opt. Express* **16** 17060
[21] Brown R H and Twiss R Q 1956 *Nature* **178** 1046
[22] Kaneda F, Garay P K, U'Ren A B and Kwiat P G 2016 *Opt. Express* **24** 10733
[23] Jin R B, Wakui K, Shimizu R, Benichi H, Miki S, Yamashita T, Terai H, Wang Z, Fujiwara M and Sasaki M 2013 *Phys. Rev. A* **87** 063801